Semi-Mechanistic Model to Characterize Non-Linear Pharmacokinetic of Nimotuzumab in Patients with Advanced Breast...

Article *in* The Journal of Clinical Pharmacology · March 2015

DOI: 10.1002/jcph.496

CITATION
1

READS
107

9 authors, including:

Mayra Ramos-Suzarte
Biotech Pharmaceuticals Co.,Ltd. BDA, Beijin...
94 PUBLICATIONS **840** CITATIONS
SEE PROFILE

Concepcion Peraire
University of Barcelona
57 PUBLICATIONS **479** CITATIONS
SEE PROFILE

Gilberto Castañeda-Hernández
Center for Research and Advanced Studies of...
230 PUBLICATIONS **2,874** CITATIONS
SEE PROFILE

Niurys de Castro Suarez
University of Havana
4 PUBLICATIONS **32** CITATIONS
SEE PROFILE

The Journal of Clinical Pharmacology
2015, XX(XX) 1–11

DOI: 10.1002/jcph.496

Semimechanistic Model to Characterize Nonlinear Pharmacokinetics of Nimotuzumab in Patients With Advanced Breast Cancer

Leyanis Rodríguez-Vera, MSc[1], Mayra Ramos-Suzarte, PhD[2], Eduardo Fernández-Sánchez, PhD[3], Jorge Luis Soriano, MD, PhD[4], Concepción Peraire Guitart, PhD[5], Gilberto Castañeda Hernández, PhD[6], Carlos O. Jacobo-Cabral, PhD[6], Niurys de Castro Suárez, MSc[1], and Helena Colom Codina, PhD[5]

Abstract

This study aimed (1) to develop a semimechanistic pharmacokinetic (PK) model for nimotuzumab in patients with advanced breast cancer and (2) to identify demographic, biochemical, and clinical predictive factors of the PK variability. Data from a phase 1 study were analyzed using the nonlinear mixed-effects approach (NONMEM). A target-mediated disposition model that included 2 open PK compartments, the monoclonal antibody (mAb)–target binding, and target and mAb–target complex turnovers best described the linear and nonlinear PK. Covariates had no influence on the PK parameters. The final parameter estimates were 19.93 L (steady-state volume), 0.0045–0.0172 L/h (range of total clearance values), 6.96 μg/mL (steady-state binding constant), 5.50 h^{-1} (target degradation rate constant), 1.43 (μg/mL) · h^{-1} (complex formation rate), and 0.148 h^{-1} (complex internalization rate constant). The model described the effect of the mAb–target binding, and target and mAb–target complex turnovers on nimotuzumab PK. Simulations showed that doses above 200 mg maintained the 50% target occupancy during all of the treatment. This model can be very useful for knowing the dosing schedules required for efficacy and supports further investigation of the pharmacokinetic/pharmacodynamic relationships of nimotuzumab to improve its therapeutic use.

Keywords

breast cancer, EGFR, nimotuzumab, semimechanistic, NONMEM

Nimotuzumab is a humanized monoclonal antibody (mAb), developed at the Center of Molecular Immunology (Havana, Cuba). It is a genetically engineered IgG1 with intermediate affinity for the epidermal growth factor receptor (EGFR).[1] Nimotuzumab blocks EGFR–ligand interactions and subsequent signal transduction events.[2,3] The biologic consequences of this interaction are potent antiproliferative, antiangiogenic, and proapoptotic activities affecting epithelial tumors that overexpress EGFR (ie, head-neck, breast, and colorectal cancers).[4–9] Another antitumor mechanism is antibody-dependent cellular cytotoxicity.[10]

Earlier studies of patients with advanced solid tumors characterized the pharmacokinetics (PK) of nimotuzumab, either by noncompartmental[11–13] or classical compartmental analyses.[4] In all the cases, after nimotuzumab intravenous infusion at doses ranging from 50 to 400 mg, nonlinear pharmacokinetic behavior was reported. However, the empirical description of nonlinear kinetics provided by the noncompartmental approach is by itself insufficient to fully characterize mAb–target interactions.[14] Based on the knowledge of its mechanism of action,[1] the nonlinear PK previously reported,[11] could be because of the interaction of nimotuzumab with its pharmacological target (EGFR) and of the limited amount of this target relative to nimotuzumab. As with other anti-EGFR mAbs, nimotuzumab is known to be mainly eliminated by 2 different processes, (1) nonlinear or target-mediated elimination, particularly evident at low

[1]Laboratory of Pharmacokinetic, Department of Pharmacology & Clinical Pharmacy, Institute of Pharmacy & Foods, University of Havana, Havana, Cuba
[2]Center of Molecular Immunology, Havana, Cuba
[3]Center for Biological Evaluation and Research, Institute of Pharmacy & Foods, University of Havana, Havana, Cuba
[4]Hermanos Ameijeiras Hospital, Havana Center, Havana, Cuba
[5]Pharmacy and Pharmaceutical Technology Department, School of Pharmacy, University of Barcelona, Barcelona, Spain
[6]Department of Pharmacology, CINVESTAV-IPN, Mexico City, Mexico

Corresponding Author:
Leyanis Rodríguez-Vera, MSc, Professor of Pharmacokinetics. Institute of Pharmacy and Foods, University of Havana, 222 St. and 23 Avenue, La Coronela, La Lisa, Havana, Cuba CP 13600
Email: leyanis@ifal.uh.cu

concentrations, consisting of endocytosis followed by internalization of cell surface receptors; and (2) linear elimination, dominant at high concentrations, when the nonlinear pathway is saturated.[1]

Although classical compartment pharmacokinetic models with parallel linear and nonlinear elimination processes, can capture the dose-dependent kinetics, they do not account for nonlinear distribution processes, and they assume apparent volumes are independent of dose.

Mager and Jusko[15] proposed a general mechanistic model, first introduced by Levy in 1994,[16] to describe the PK of monoclonal antibodies exhibiting target-mediated disposition (TMD). In brief, this model explicitly considers mAb–target binding as part of the model. However, the concentrations of the target and of the mAb–target complex are either frequently unavailable or, if available, insufficient to describe the initial binding process, so that this model becomes unidentifiable in most cases. That is why some simplifications from the general model, such as those assuming rapid binding quasi-equilibrium models, quasi-steady-state models, and Michaelis-Menten models, have been proposed with a reduced number of parameters to be estimated.[17–19]

A semimechanistic TMD model for nimotuzumab would contribute to confirming its target interaction-based disposition, and it would be a very helpful tool for designing future studies and investigating pharmacokinetic-pharmacodynamic relationships.

The objectives of this study were (1) to develop for the first time a semimechanistic target-mediated disposition model for nimotuzumab, to describe its pharmacokinetics, target binding, and target saturation, using the population pharmacokinetic approach in patients with breast cancer; and (2) to identify demographic, biochemical and clinical factors predictive of nimotuzumab's pharmacokinetic variability.

Methods

Study Design and Patient Eligibility

Data from a single-center phase 1 clinical trial, were used for the population PK analysis. The Cuban clinical trial register number was RPCE00000057,[20] which coincided with the number of the register of the World Health Organization.[21] Twelve patients were included in 4 treatment cohorts corresponding to 50-, 100-, 200-, and 400-mg weekly doses of nimotuzumab. Three patients per dose level were enrolled. Patients with histologically confirmed advanced-stage breast local epithelial tumors that were not amenable to receiving further therapy and who had finished their last treatment at least 4 weeks before were included in the trial. Other selection criteria were good performance status and normal hematological conditions, as well as normal hepatic and renal function. The most important exclusion criteria were previous treatment with murine anti-EGFR antibodies, pregnancy or lactation, serious chronic diseases, and active infections. All patients signed a written consent form before their inclusion in the clinical trial.

The following data were collected from the patients on days 0, 5, 26, 47, and 68 from the start of the treatment (day 0): demographic characteristics, comedication, biochemical and hematological measurements (hemoglobin, hematocrit, creatinine, aspartate aminotransferase [AST], alanine aminotransferase [ALT], alkaline phosphatase, total protein, and albumin).

Nimotuzumab was administered weekly for 2.5 months by intravenous infusions of 0.5 hours. Patients received a total of 10 doses on days 0, 7, 14, 21, 28, 35, 42, 49, 56, and 63 of the treatment. Patients were also treated with $60\,mg/m^2$ of doxorubicin and $600\,mg/m^2$ of cyclophosphamide every 21 days, on days 8, 28, 49, and 70. More details about the treatment are given elsewhere.[11] The trial was conducted under the principles outlined in the Declaration of Helsinki. The Ethics Review Committee for human subjects' protection in clinical trials at the Hermanos Ameijeiras Hospital and the State Center for Drug Quality Control and the National Regulatory Agency, approved the protocol.

Serum Sampling Schedule and Assay Method

Serum samples were collected before the start (0 hours) and at the end of intravenous infusion (0.5 hours) on days 0, 7, 14, 21, 28, 35, 42, 49, 56, and 63 of the treatment. Additional samples were taken after the first (day 0) and the 10th (day 63) doses. After the first dose, sampling was at 0.5 hours and 1, 2, 4, and 6 days from the start of the infusion. After the 10th dose on day 63, samples at 0.5 hours and 1, 6, 14, 20, and 26 days after the start of the infusion were obtained. Samples were allowed to clot and then were centrifuged. Serum was collected and stored at $-20°C$. Serum concentrations of nimotuzumab were determined by a validated enzyme-linked immunosorbent assay. The recombinant extracellular of EGFR domain captured nimotuzumab from serum samples. Bound nimotuzumab was detected with an alkaline phosphate–labeled anti-human IgG conjugate (A-3188; Sigma Chemical). Para-nitro-phenyl-phosphate diluted in diethanolamine buffer was used as the substrate for color development to quantify serum nimotuzumab against a standard curve (ranged from 0 to 500 ng/mL in a 2-fold serial dilution). Absorbance was read at 405 nm. The lower limit of quantification of nimotuzumab in human serum was 7.8 ng/mL. The imprecision was less than 10%, and the accuracy was of 98.23%.The linear range of the assay was 7.8–500 ng/mL.

Population Pharmacokinetic Analysis

A simultaneous analysis of all the log-transformed concentrations-versus-time values found after the 4

assayed dose regimens (50–400 mg) was performed with the nonlinear mixed-effects models implemented in NONMEM software, version 7.2.[22] The first-order estimation method with interaction was used throughout the entire modeling process. Initially, the full TMD model, proposed by Mager and Jusko[15] and describing the pharmacokinetics as a combination of a linear disposition process and nonlinear process involving the target was selected. Approximations from this model were also applied.[19] Briefly, the full TMD model explicitly considered the binding equilibrium between free mAb and free target concentrations in the central compartment, as the free target and the mAb-target complex turnovers. Between-patient variability (BPV) was tested in all the PK parameters; meanwhile, between-occasion variability (BOV)[23] was tested only in clearance. Both (BPV and BOV) were modeled exponentially assuming a log-normal distribution. Residual error as an additive error on log-transformed data was applied. To statistically distinguish between nested models the likelihood ratio test based on the reduction of the minimum objective function value (MOFV), was used (ΔMOFV: -2 log likelihood, approximate χ^2 distribution). A ΔMOFV of 7.879 units for 1 degree of freedom corresponding to $P \leq .005$ was considered statistically significant. For non nested models, the model selection was based on the AKAIKE information criterium (AIC). The model with the smallest value of AIC[24] was considered as the best.

Once the base model was achieved, the effect of age, body weight, albumin, race, and biochemical variables representative of liver function on PK parameters was investigated with NONMEM. Missing albumin values for some occasions in some patients (n = 6) were replaced by mean values calculated from the remaining existing values within the same patient. The covariate analysis was based on a stepwise forward inclusion followed by a stepwise backward exclusion procedure. Significance levels adopted in each case were 5% and 1%, respectively. The decrease in MOFV, physiologically meaningful parameter estimates, parameter precision, reductions in BPV, η- and ϵ-shrinkage values, successful termination of the models, and visual inspection of goodness-of-fit plots were also considered for model selection.

Model Evaluation

The nonparametric bootstrap method with replacement was used to assess the stability of the final model and to construct confidence intervals (CIs) of the pharmacokinetic parameters.[25] Two hundred data sets were reconstructed by resampling from the original data. The final model was fitted to the replicate data sets, and parameter estimates for each of the replicate data sets were obtained. The mean values of the parameters obtained were compared with those estimated from the original data. The lower and upper limits of the 95%CI for each parameter accounted for its corresponding variability.

Internal evaluation of the predictive ability of the model was based on prediction-corrected visual predictive checks constructed from 1000 simulated replicates of the original data set. For that purpose, the 95% prediction interval of the 2.5th, 50th, and 97.5th percentiles of the simulated data were calculated and plotted together with the corresponding percentiles calculated from the raw data. The 2.5th, 50th, and 97.5th percentiles of the raw data should be within the corresponding 95% prediction intervals of the simulated data.

Model-Based Simulations

Once the model was validated, simulations were performed to investigate the influence of different doses on the pharmacokinetics of nimotuzumab. The population values of the parameters were fixed to their final estimates. Concentrations achieved over 5 months after weekly nimotuzumab doses of 50, 100, 200, 400, and 1200 mg were simulated, and the corresponding median area under the curve (AUC) values and 95% confidence intervals for each dose were calculated.

Results

Patients and Data Collection

A total of 443 serum concentration-versus-time data from 12 patients were included in the population PK analysis. From those, 84 belonged to occasion 1, 288 to occasions 2–9, and 71 to occasion 10. Table 1 summarizes the demographic and biochemical characteristics of the patients included in the analysis.

With the exception of albumin concentrations, the biochemical parameters were within the normal expected ranges in all patients. A tendency to lower albumin mean values (mean, 35.1 ± 6.7 g/L with fluctuations within each patient, from the start until the end of treatment) than those expected as normal (43 g/L) were found. Patients showed similar body weights and ages, and they were around the population means.

Population PK Model

The full TMD model[15] could not be captured by the data, probably because of the absence of target or mAb–target complex concentrations, crucial for estimation of the second-order binding (k_{on}) and the first-order dissociation (k_{off}) rate constants. As recently reported in the literature, the target-binding process was approximated by a quasi-steady-state approximation (QSS), in which the binding rate was balanced by the sum of dissociation and internalization rates.[19] The schematic of the QSS approximation is shown in Figure 1. The linear disposition was described by 2 PK compartments—central and tissue compartments (distribution volumes, V_c and V_t),

Table 1. Demographic and Biochemical Characteristics of Patients Included in the Population PK Analysis (n = 12 Women)

Patient Characteristics (Units)	Mean (Standard Deviation)
Age (years)	49.7 (10.23)
Body weight (kg)	65.1 (7.53)
Hemoglobin (g/dL)	12.9 (0.66)
Hematocrit	0.4 (0.02)
Creatinine (μmol/L)	72.8 (23.60)
AST (μ/L)	14.0 (4.70)
ALT (μ/L)	11.5 (6.33)
Alkaline phosphatase (μ/L)	176.1 (41.83)
Total protein (g/L)	66.6 (7.01)
Albumin (g/L)	35.1 (6.7)
Race	
White, n (%)	8 (66.66)
Black, n (%)	4 (33.33)
Histology	
Ductal carcinoma, n (%)	11 (91.66)
Lobular carcinoma, n (%)	1 (8.33)
Degree of differentiation	
Intermediate-malignancy grade, n (%)	2 (16.66)
High-malignancy grade, n (%)	8 (66.66)
Low-malignancy grade, n (%)	2 (16.66)

Data given as mean (standard deviation) or counts, n (percentage).
AST, aspartate aminotransferase; ALT, alanine aminotransferase.

with first-order exchange between them (distributional clearance [CL_D]) and first-order elimination from the central compartment (clearance [CL]). The mAb molecules in the central compartment were binding to the free target molecules (steady-state rate constant [K_{ss}]). Before dosing, the target was at dynamic equilibrium between zero-order kinetic synthesis (k_{syn}) and degradation at a rate of k_{deg}. The antibody–target complexes were irreversibly internalized at a rate or k_{int}. Between-patient variability was associated with CL, V_c, and K_{ss}. Between-occasion variability could not be included.

The system was defined in terms of total mAb ($C_{tot} = C + RC$) and total target ($R_{tot} = R + RC$) concentrations, and the measurable free concentrations (C) were calculated through equation 1.

$$C = 0.5 \cdot \left[Ctot - Rtot - Kss + \sqrt{(Ctot - Rtot - Kss)^2 + 4 \cdot Kss \cdot Ctot} \right] \quad (1)$$

The set of ordinary differential equations derived describing the mAb kinetics and turnover processes of the receptor was the following:

$$\frac{dC_{tot}}{dt} = -(Kel + kpt) \cdot C + ktp \cdot \frac{At}{V} - \left(\frac{kint \cdot Rtot \cdot C}{kss + C} \right) \quad (2)$$

$$\frac{dAt}{dt} = kpt \cdot C \cdot Vc - ktp \cdot At \quad (3)$$

$$\frac{dRtot}{dt} = ksyn - kdeg \cdot Rtot - \left(\frac{(kint - kdeg) \cdot C \cdot Rtot}{Kss + C} \right) \quad (4)$$

where C_{tot} and C are the total and free mAb concentrations; At is the amount of the free mAb in tissue compartments: R_{tot}, R, and RC_{tot} are the concentrations of the total target, free target, and mAb–target complex, respectively, in the central (serum) compartment; k_{el}, k_{pt},

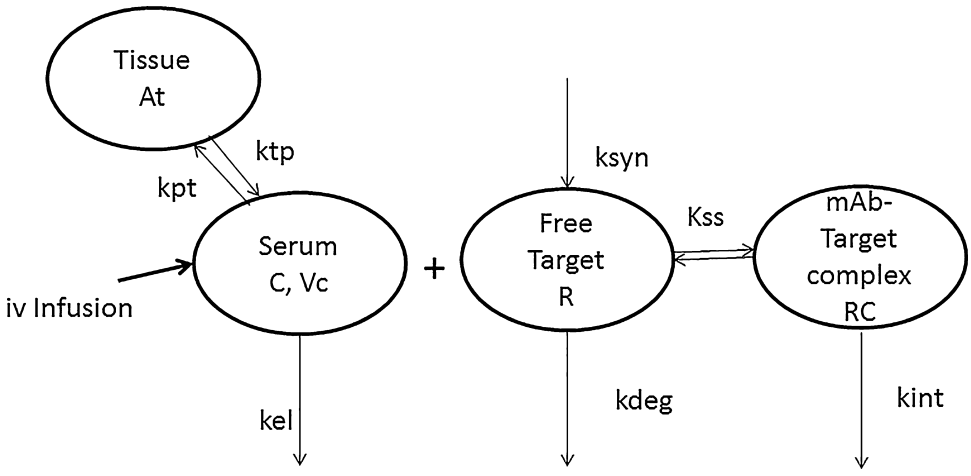

Figure 1. Schematic representation of the QSS approximation of the target-mediated disposition model, which explicitly includes mAb-target binding in central compartment, receptor turnover and internalization of the mAb-target complex. K_{el}, first-order mAb elimination rate constant; k_{pt}, first-order serum-tissue distribution rate constant; k_{tp}, first-order tissue-serum distribution rate constant; At, amount of the mAb in the tissue compartment; C, concentration of free mAb in the serum compartment; R, concentration of free target; RC, concentration of the mAb-target complex; k_{syn}, synthesis rate constant of the target; k_{deg}, degradation rate constant of the target; k_{int}, internalization rate constant of the mAb-target complex; K_{ss}, steady-state rate constant.

and k_{tp} are the linear elimination, serum-to-tissue distribution, and tissue-to-serum distribution rate constants, respectively. The model was concluded successfully, but the standard errors could not be estimated because the matrix was algorithmically singular. This could be because of overparameterization. Therefore, a simpler QSS approximation with constant target concentrations and 1 less parameter was tested. However, it did not provide physiologically meaningful parameter values, particularly for K_{SS}, which had a much higher nimotuzumab value (about 200 μg/mL) than the "in vitro" K_D reported values (1.5×10^{-4} μg/mL).[1] The QSS approach, with nonconstant total target concentrations, provided meaningful values of parameter estimates, and it was retained as the best base model. It was parameterized in terms of CL, V_c, CL_D, V_t, K_{ss}, k_{int}, k_{syn}, and k_{deg}. In this model, the total systemic clearance (CL_T) was estimated by equations 5–7.

$$CL_T = CL_{linear} + CL_{non-linear} \quad (5)$$

$$CL_{linear} = kel \cdot Vc \quad (6)$$

$$CL_{non-linear} = \frac{kint \cdot Rtot}{Kss + C} \cdot Vc \quad (7)$$

Any of the covariates (ie, body-weight, serum albumin concentration, age, and race on both CL and V_c and liver function parameters on CL) had statistically significant effects on PK parameters. Accordingly, the early-developed base model was selected as the final one. Figure 2 shows the observed and population-predicted nimotuzumab concentrations versus time after the first and tenth doses. In general the final model adequately described the trend of observed data at steady state for most doses (ie, after the 10th dose, occasion 10). Conversely, under- and overpredictions were observed at 50 and 200 mg, respectively, after the first dose (occasion 1). The goodness-of-fit plots shown in Figure 3 suggest an acceptable description of the data.

The final parameter estimates and their 95% confidence intervals are summarized in Table 2. The BPV values associated with CL, V_c, and K_{ss} were of 11.31%, 50%, and 87.86%, respectively. A residual error value of 48% was obtained. The parameter values generated from the bootstrap analysis were, in most cases, similar to those of the model developed using the 12 patients. The percentage of difference between the final population estimates and mean values from bootstrap sampling was lower than 17% for all the structural pharmacokinetic and random-effect parameters, with the exception of CL (38.84%), k_{deg} (33.27%), and k_{int} (52.63%), estimated with lower precision. All final model parameter estimates lay within the 95%CI obtained by the bootstrap method.

Table 3 summarizes the mean ± standard deviation values of predicted linear, nonlinear and total clearances for each group of treatment.

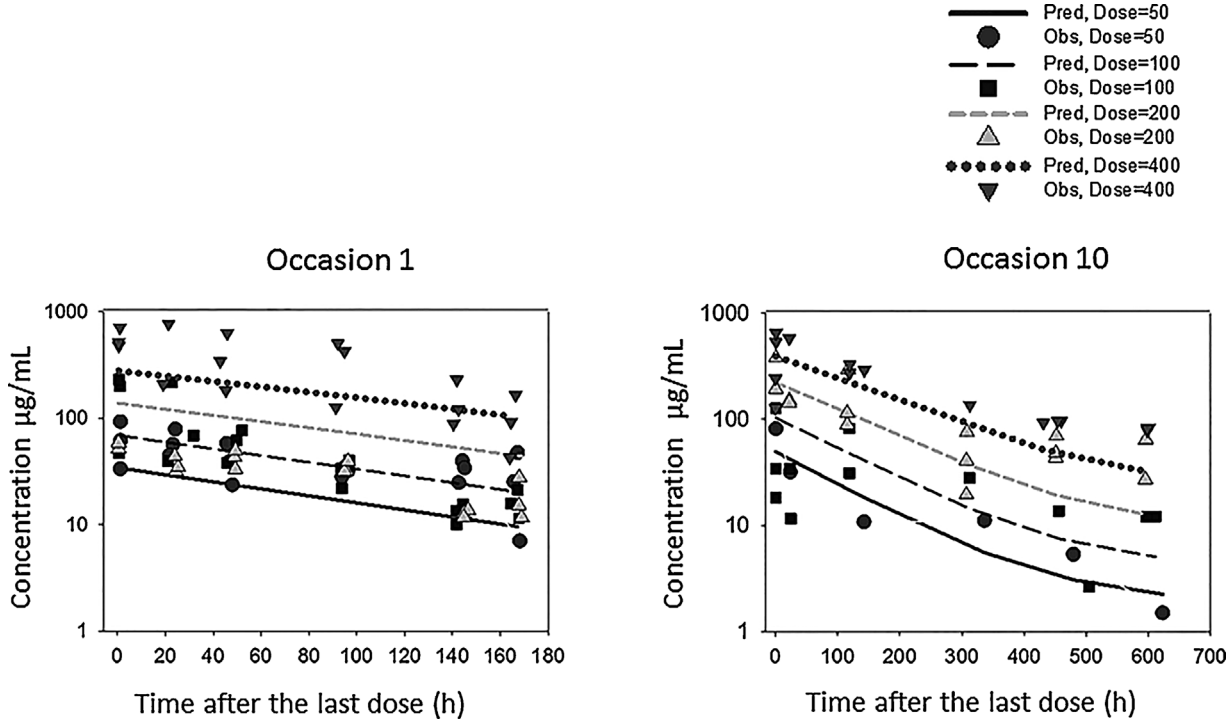

Figure 2. Superimposed observed (OBS) and population predicted (PRED) concentrations of nimotuzumab (micrograms per milliliter) versus time after the last dose administered (hours) for 50-, 100-, 200-, and 400-mg doses on occasions 1 (a, left) and 10 (b, right).

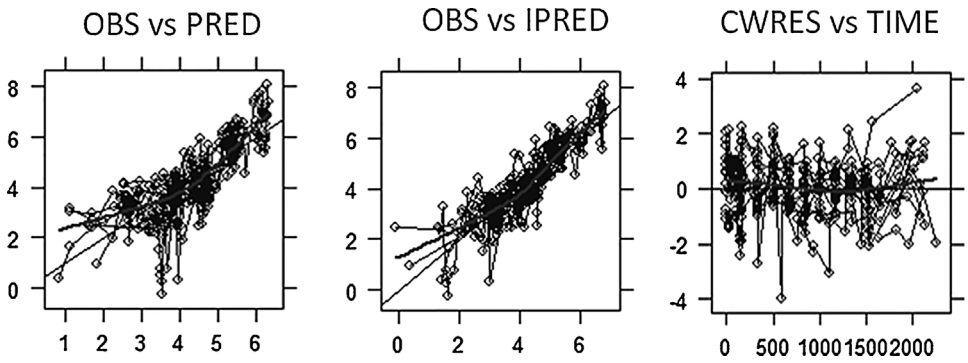

Figure 3. Goodness-of-fit plots for the final population PK model. Left: plot of population predictions (PRED) versus observed nimotuzumab concentrations (OBS); thin line, identity line; thick line, general trend of the data. Middle: plot of individual Bayesian predictions versus observed nimotuzumab concentrations (thin line, identity line; thick line, general trend of the data). Concentrations (DV, PRED, and IPRED) expressed in micrograms per milliliter given as ln values; time given in hours. Right: plot of conditional weighed population residuals (CWRES) versus time from the start of the treatment, (thin line, the line $y = 0$; thick line, smooth line indicating the general trend of the data).

The total systemic clearance calculated from the contribution of the linear and the nonlinear elimination pathways resulted in values of 0.0045 L/h (50 mg), 0.0172 L/h (100 mg), 0.0063 L/h (200 mg), and 0.0055 L/h (400 mg). The contribution of the linear elimination pathway to the total clearance was very low (from 2.80% to 10.40%) when compared with that of the nonlinear pathway, which accounted for 91.56%–97.33% of the total elimination process. A trend to lower nonlinear clearance values with increased doses, particularly from 100 to 400 mg, was observed (CL values from 0.0167 to 0.0051 L/h, respectively). Meanwhile the linear clearance values remained almost constant across increasing doses (0.00047–0.00048 L/h), but its contribution to the total clearance values increased from 2.8% (100 mg) to 8.6% (400 mg). The reduction of nonlinear clearance of nimotuzumab from doses of 100 to 400 mg was about 70%.

Table 2. Pharmacokinetic Parameter Estimates for the Final Model

Parameters (Units)	Estimate	Mean (95%CI) Bootstrap Results
Disposition PK parameters		
CL ($L \cdot h^{-1}$)	0.000703	0.00043 (0.0000868–0.00139)
V_C (L)	1.43	1.38 (1.09–1.81)
V_t (L)	18.5	21.47 (7.91–209.10)
CL_D ($L \cdot h^{-1}$)	0.00322	0.0033 (0.0021–0.0051)
K_{ss} ($\mu g/mL$)	6.96	7.40 (1.04–150.40)
k_{int} (h^{-1})	0.148	0.226 (0.017–2.664)
k_{syn} ($\mu g/mL) \cdot h^{-1}$	1.43	1.46 (0.71– 3.29)
k_{deg} (h^{-1})	5.50	7.33 (2.05–74.21)
$t_{1/2\beta}$ (h)	483.71	–
Between-patient variabilities[a]		
BPV_{CL} (%)	11.31	10.82 (0.64–33.54)
BPV_{Vc} (%)	50.00	51.03 (19.70–75.61)
BPV_{Kss} (%)	87.86	83.42 (39–131)
Residual error		
$RE_{additive\ on\ log\text{-}data}$ (%)	48.00	47.98 (33.09–69.92)
Shrinkage		
η-shrinkage (%)	9.55	
ϵ-shrinkage (%)	3.53	

Standard errors of parameter estimates were not provided by the program because of matrix algorithmically singular. CL, clearance; V_c and V_t, central and tissue distribution volumes, respectively; V_{ss}, total distribution volume at steady state: $Vc + Vt = 19.93$ L; CL_D, distributional clearance; K_{ss}, concentration of the drug at which the interaction with target is half maximal or steady-state constant; k_{int}, k_{syn}, and k_{deg}, internalization, target production and target degradation rate constants, respectively; CI, confidence interval.

[a]BPV, between-patient variability; RE, residual error. BPV and RE are expressed as coefficients of variation (%).

Model Evaluation

The prediction-corrected visual predictive check showed the acceptable predictive capability of the model. As shown in Figure 4, the 2.5th, 50th, and 97.5th percentile lines of the observations fell inside the areas of the 95%CI of the corresponding percentiles for the simulated data.

To better appreciate the differences between linear elimination kinetics, Michaelis-Menten elimination kinetics, and target-mediated disposition models, predicted values by each model were superimposed, shown in Figure 5, and compared. According to this, when compared with the TMD model fit, the linear elimination model predicted slower clearance from the dose of 50 to 200 mg and was similar for the highest dose with parallel concentration-versus-time decays. The Michaelis-Menten elimination model predicted faster clearance from 50 to 100 mg, was similar for the dose of 200 mg, and was slower for the highest dose. This agrees with the finding that when mAb binding to the target is not saturated, which occurs at doses from 50 to 200 mg, the nonlinear elimination pathway is the major contributor to the nimotuzumab elimination, resulting in faster clearance than that predicted

Table 3. Mean ± SD Values of Linear, Nonlinear, and Total Clearance for Each Treatment Group (50–400 mg)

Dose (mg)	CL Linear (L/h)	CL Nonlinear (L/h)	CL Total (L/h)
50	0.00047 ± 0.000001	0.00412 ± 0.00148	0.00459 ± 0.00148
100	0.00048 ± 0.000003	0.01674 ± 0.00634	0.01721 ± 0.00634
200	0.00047 ± 0.000004	0.00591 ± 0.00220	0.00638 ± 0.00221
400	0.00047 ± 0.00002	0.00508 ± 0.00238	0.00554 ± 0.00238

by a linear elimination process. Otherwise, at the highest doses (400 mg), when the mAb–target complex can be saturated, the linear clearance pathway is controlling the concentration–time profile kinetics, and the contribution of the nonlinear pathway becomes negligible.

Simulations

Figure 6a shows the mean predicted concentrations-versus-time profiles from the final model after weekly doses of 50, 100, 200, 400, and 1200 mg of nimotuzumab over 5 months. More expanded views of the predicted concentrations after the last doses for each dose regimen are also displayed in Figure 6b. Figure 6c depicts the free receptor concentration-versus-time profiles predicted by the model after each dose regimen.

The more expanded timescale after the 10th dose allowed to appreciate better the nonlinear behavior within the range of simulated doses. Median AUC values and the corresponding 95% CIs estimated from each simulation were of 6624 (767.8–17 581), 14 121 (1685–35 949), 30 685 (4017–74 732), 75 296 (11 351–167 519), and 316 633 (82 546-634 575) μg/mL · h for the doses of 50, 100, 200, 400, and 1200 mg, respectively.

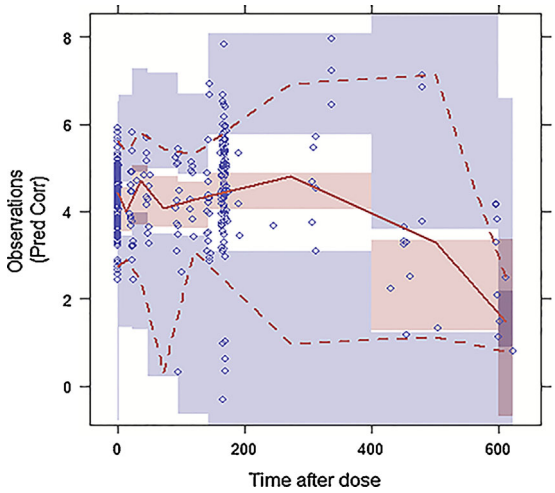

Figure 4. Prediction-corrected visual predictive checks corresponding to serum concentrations (given as ln values of concentrations expressed as micrograms per milliliter) versus time (time after the last dose given, in hours) profiles. Median (solid line) and 97.5th and 2.5th percentiles (dashed lines) of the observations, as well as the 95% confidence intervals (CIs) for the median and 2.5th and 97.5th percentiles of the simulated data (covered by the light red and blue areas, respectively) are superimposed in each graph. The 2.5th, 50th, and 97.5th percentile lines of the observations fell inside the areas of the corresponding 95%CI.

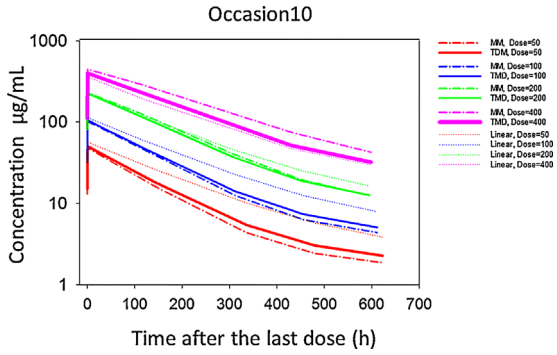

Figure 5. Superimposed predicted concentrations versus time on occasion 10, after fitting of linear elimination, Michaelis-Menten elimination, and target-mediated disposition models to the data of the current study. Solid lines, TMD model; dashed-dotted lines, Michaelis-Menten elimination kinetics; dotted lines, linear elimination kinetics.

Discussion

This is the first time that a semimechanism-based population pharmacokinetic model has been developed for nimotuzumab after repeated intravenous administration in breast cancer patients. The model describes the target-mediated disposition of the antibody, and it goes beyond the simple empirical description of nimotuzumab's nonlinear pharmacokinetics.[14,19,26] Conversely, capacity-limited elimination described by Michaelis-Menten kinetics, has been applied for other mAbs and recognized by the same pharmacological target as nimotuzumab (EGFR).[27–29] The more complex TMD approach has led to a better understanding of the influence of mAb–target binding and of the target and complex turnover rates on the pharmacokinetics of nimotuzumab.

The clearance of mAbs such as nimotuzumab targeting cell surface receptors can be greatly accelerated by a target-mediated process that results in dose-dependent nonlinear kinetics as reported for nimotuzumab.[11] Because a simple PK model did not fully characterize the PK of nimotuzumab, the TMD model was built. Although some inconsistencies in the data were found, the PK profiles suggested that the mAb is rapidly removed from circulation because of its binding to EGFR, which is highly expressed in the tumor tissues. This binding is saturated at the highest doses (from 200 to 400 mg). Moreover, a dose-dependent reduction was observed in the volumes of distribution at steady state.[11] The exposures achieved at steady state, after the 10th administration of each dose regimen were, in general, higher than those after the first, suggesting that the

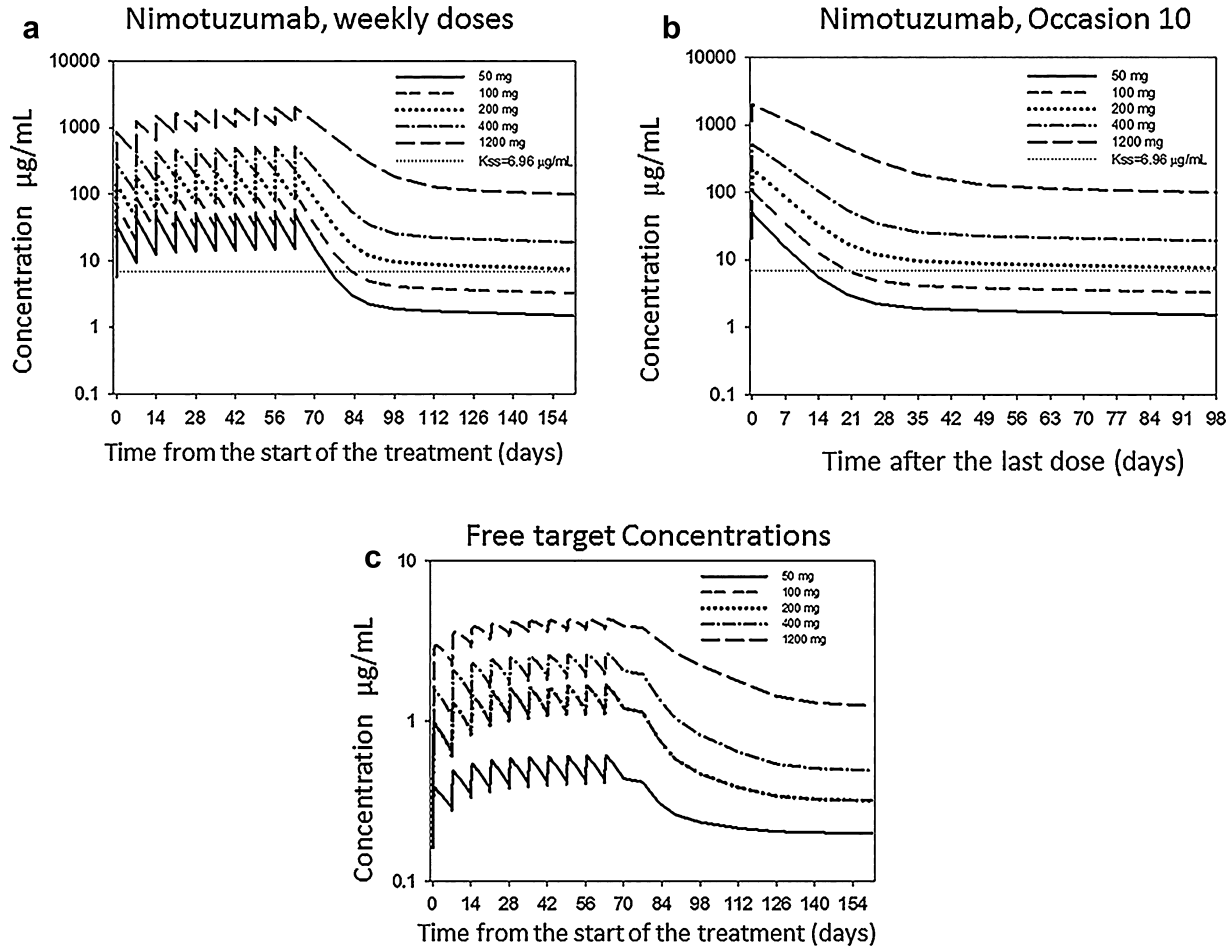

Figure 6. Predicted concentrations from the final model. (a) Predicted concentrations from the start of the treatment with weekly doses of 50, 100, 200, 400, and 1200 mg during 5 months. (b) Predicted concentrations after the last administration on day 63 (occasion 10) of treatment with weekly doses of 50-1200 mg. (c) Free target predicted concentrations from the start of the treatment with weekly doses of 50, 100, 200, 400, and 1200 mg during 5 months.

targets were still occupied when theses administrations were performed.

The model developed involved 2 open PK compartments, the turnover processes of the EGFR, and the internalization of the nimotuzumab–EGFR complex, assuming a mAb–target association rate much faster than that of the remaining processes. In general, the model fitted the observed data reasonably, particularly at steady state, and offered a plausible explanation of the nimotuzumab PK. However, as indicated above, some inconsistencies were found for the 50-mg (underpredicted) and 200-mg (overpredicted) dose groups after the first dose. The reasons for these biases are unknown. It could be several factors, such as high levels of shed EGFR,[30] EGFR polymorphism,[31] and differences in EGFR expression.[32] In the current study, immunogenicity was discarded because the human antimurine antibody response did not alter the clearance of nimotuzumab.[11] Model validation by prediction-corrected visual predictive checks showed that the selected model was adequately captured by the observed data.

Physiologically, meaningful PK parameters were obtained. The nonlinear clearance accounted for most of the total elimination process: 91.56%–97.33%. The total nimotuzumab clearance values ranged from 0.0045 to 0.0172 L/h or equivalently from 0.1080 to 0.413 L/day. These values were similar to those reported for endogenous IgG (0.21 L/day).[31] They were also in line with the total clearance reported for other anti-EGFR mAbs such as panitumumab[27] (0.273 L/day) and trastuzumab[33] (0.225 L/day). Conversely, cetuximab[28] (1.42 L/day) and matuzumab[29] (2.83 L/day) showed clearance values about 3 and 6 times higher, respectively, than that of nimotuzumab.

The distribution volume at steady state ($V_{ss} = V_c + V_t$) was 19.93 L (for a mean body weight of 65 kg),

suggesting an apparently limited distribution outside the vascular space, or the extracellular volume. This value was larger than those of cetuximab ($V_{ss} = 5.26$ L for a 60-kg patient)[28] and matuzumab ($V_{ss} = 5.57$ L for a 71-kg patient),[29,34] which are approximately equal to the plasma volume.

A higher K_{ss} value (6.96 μg/mL) than the equilibrium dissociation rate constant (K_D) from "in vitro" studies (1.5×10^{-4} μg/mL or 10^{-9} mol/L)[1] was found. The incorporation of target turnover and mAb–target internalization kinetics in the model, could account for these differences. In the current study, the target was estimated to have a more rapid turnover ($K_{deg} = 5.50$ h^{-1}, 7.56 minutes of half-life) compared with the timescale of the other processes. It was faster than the antibody-target internalization ($K_{int} = 0.148$ h^{-1}, half-life, 4.68 hours) and also than the mAb half-life (483.71 hours or 20.15 days). The nimotuzumab half-life (20.15 days) is in line with those reported for IgG1, IgG2, and IgG4 subclasses (21 days)[31,35,36] and also consistent with that found for trastuzumab (28 days) in a population pharmacokinetics study in patients with breast cancer.[33] The rapid renewal of the target makes it difficult to be saturated even if present at low concentrations. Moreover, the internalization process is not negligible ($K_{int} = 0.148$ h^{-1}), so that it could also contribute to these differences, given that $Kss = (K_{int} + K_{off})/K_{on}$. The subsequent observed K_{ss} value suggests that concentrations around 6.96 μg/mL can yield 50% of free receptors at steady state, and it could be used as the starting point to guide an efficacious dosing schedule. In the current study, the largest doses of nimotuzumab (weekly 200–400 mg) resulted in a lesser contribution of the nonlinear clearance pathway. This was because of the saturable target-mediated mAb clearance subsequent to the intermediate-affinity binding of nimotuzumab to the EGFR. For this reason, we speculate that doses above this critical range of 200–400 mg would not lead to greater occupancy of the EGFR, so that, it could result in less efficient usage of this monoclonal anti-EGFR antibody in cancer therapy. In addition, higher percentages of the given doses would be eliminated by the linear pathway, with potentially bad consequences for patient safety. In line with these considerations, simulations of weekly doses from 50 to 1200 mg of nimotuzumab during 5 months (Figure 6a) showed that doses from 200 to 1200 mg would assure 50% receptor occupancy overall during the treatment period.

None of the covariates (ie, age, body weight, serum albumin level, alkaline phosphatase, creatinine, AST, ALT, and total protein) showed a statistically significant influence on the PK parameters, so that large between-patient variability was still to be explained, particularly for V_c and K_{ss} (CL, V_c, and K_{ss} BPV values of 11.31%, 50%, and 87.86%, respectively). This could be because of the small number of patients included in the analysis and the narrow ranges of variation within these covariates. Most of the patients showed albumin serum concentrations around the mean, but slightly lower albumin serum levels were found (35.1 ± 6.7 g/L) compared with those of the cetuximab (39 g/L)[28] or trastuzumab (39 g/L)[33] population analyses. According to Fasanmade et al,[37] albumin levels can be surrogate markers of the abundance of neonatal Fc receptor (FcRn) protein, because both albumin and IgG are protected from catabolism and recycled by FcRn.[37] Although albumin serum concentrations have been shown to influence the PK of other mAbs such as infliximab,[37] in our case, they were not shown to have a significant influence on nimotuzumab clearance. Therefore, low albumin levels were not indicative of a decreased number of FcRns, and no increased linear elimination process should be expected.

Nimotuzumab was coadministered in combination with doxorubicin and cyclophosphamide, which is deemed immunogenic chemotherapy.[38] Recent findings showed that combined doxorubicin and cyclophosphamide therapy gives rise to immunogenic tumor cell death, enhances recognition, and allows phagocytosis of apoptotic debris, maturation of dendritic cells, and processing and presentation of tumor-associated antigens (ie, EGFR). Altogether, these events lead to the induction of an antitumor immune response, involving $CD4^+$ and $CD8^+$ T lymphocytes, resulting in complete eradication of tumor cells. These agents have also been reported as responsible for target overexpression,[38] so that, higher nimotuzumab clearance values should be expected at the highest concentrations. This could result in lower exposure values, contrary to what was observed after the last dose, when patients had yet been exposed to doxorubicin and cyclophosphamide.

On the other hand, Garrido and coworkers[39] demonstrated that nimotuzumab requires bivalent binding for stable attachment to the cellular surface, leading to nimotuzumab selectively binding to cells that show moderate to high EGFR expression. Because of its intermediate affinity, nimotuzumab requires the avidity conferred by bivalent binding for effective attachment, which can only occur if target density is elevated.[39] The combination of nimotuzumab with agents that increase EGFR expression can result in potential antitumoral synergism. These are issues to be considered for pharmacokinetic/pharmacodynamic model development in the future. As previously reported,[39] tumor response is depending on nimotuzumab exposure, so that such a model could allow the establishment of the target exposure to achieve the optimal response. This could be the first step for the applicability of the developed model, as a support tool for dosing individualization during clinical practice, in the future.

In summary, the QSS approximation of the full TMD model characterizes the underlying mechanism of disposition of nimotuzumab well, with saturable, intermediate-affinity binding of nimotuzumab to its pharmacologic target (EGFR) responsible for the observed nonlinear pharmacokinetic behavior. This model is the first step toward improvement of the clinical use of nimotuzumab in breast cancer patients that requires an understanding of relative distribution of antibodies to target cells compared with nontarget cells and the kinetics of target occupancy related to its efficacy. This approach has led to knowing what mAb concentration and dosing schedule are required for treatment efficacy and supports further investigation of the pharmacokinetic/pharmacodynamic relationships of nimotuzumab to improve its therapeutic use.

Acknowledgments

The authors are sincerely grateful to all the patients who have contributed to the study. We thank Raquel Swanner and Idania Suárez, MSc, for the English correction of the article.

Funding

The authors have no financial or personal conflicts of interests related to this article. This study was supported by Red de Macro Universidades de América Latina y el Caribe. Leyanis Rodríguez-Vera received Red de Macro Universidades de América Latina y el Caribe grant RMU/OBSV/021/2013.

References

1. Crombet T,Casaco A, Iznaga N. h-R3. *Drugs Future.* 2003;28:847–853.
2. Mateo C, Moreno E, Amour K, Lombardero J, Harris W, Perez R. Humanization of a mouse monoclonal antibody that blocks the epidermal growth factor receptor: recovery of antagonistic activity. *Immunotechnology.* 1997;3:71–81.
3. Viloria-Petit A, Crombet T, Jothy S, et al. Acquired resistance to the antitumor effect of epidermal growth factor receptor-blocking antibodies in vivo: a role for altered tumor angiogenesis. *Cancer Res.* 2001;61:5090–5101.
4. Crombet T, Torres L, Neninger E, et al. Pharmacological evaluation of humanized anti-epidermal growth factor receptor, monoclonal antibody h-R3, in patients with advanced epithelial-derived cancer. *J Immunother.* 2003;26:139–148.
5. Crombet T, Osorio M, Cruz T, et al. Use of the humanized anti-epidermal growth factor receptor monoclonal antibody h-R3 in combination with radiotherapy in the treatment of locally advanced head and neck cancer patients. *J Clin Oncol.* 2004;22:1646–1654.
6. Rojo F, Gracias E, Villena N, et al. Pharmacodynamic trial of nimotuzumab in unresectable squamous cell carcinoma of the head and neck: a SENDO Foundation study. *Clin Cancer Res.* 2010;16:2474–2482.
7. Reddy B, Vidyasagar M, Shenoy K, et al. BIOMAb EGFRTM (Nimotuzumab/h-r3) in combination with standard of care in squamous cell carcinoma of head and neck (SCCHN). *Int J Radiat Oncol Biol Phys.* 2007;69:S450.
8. Brade A, Magalhaes J, Siu L, et al. A single agent, phase I pharmacodynamic study of nimotuzumab (TheraCIM-h-R3) in patients with advanced refractory solid tumors. Paper presented at: 2007 ASCO Annual Meeting Proceedings Part I. *J Clin Oncol.* 2007.
9. Bebb G, Smith C, Rorke S, et al. Phase I clinical trial of the anti-EGFR monoclonal antibody nimotuzumab with concurrent external thoracic radiotherapy in Canadian patients diagnosed with stage IIb, III or IV non-small cell lung cancer unsuitable for radical therapy. *Cancer Chemother Pharmacol.* 2011;67:837–845.
10. Iznaga-Escobar N, Ramirez IL, Izquierdo JC, Suarez L, Morales D, Perez-Rodriguez R. 188 Re-labeled anti-epidermal growth factor receptor humanized monoclonal antibody h-R3: labeling conditions, in vitro and in vivo stability. *Methods Find Exp Clin Pharmacol.* 2003;25:703–711.
11. Rodríguez-Vera L, Fernández-Sánchez E, Soriano JL, et al. Pharmacokinetics evaluation of nimotuzumab in combination with doxorubicin and cyclophosphamide in patients with advanced breast cancer. *J Life Sci.* 2013;7:1123–1133.
12. Strumberg D, Schultheis B, Scheulen ME, et al. Safety, efficacy and pharmacokinetics of nimotuzumab, a humanized monoclonal anti-epidermal growth factor receptor (EGFR) antibody, in patients with locally advanced or metastatic pancreatic cancer. *Int J Clin Pharmacol Ther.* 2010;48:473–475.
13. Okamoto W, Yoshino T, Takahashi T, et al. A phase I, pharmacokinetic and pharmacodynamic study of nimotuzumab in Japanese patients with advanced solid tumors. *Cancer Chemother Pharmacol.* 2013;72:1063–1071.
14. Grimm HP. Gaining insights into the consequences of target mediated drug disposition of monoclonal antibodies using quasi-steady-state approximations. *J Pharmacokinet Pharmacodyn.* 2009;36:406–420.
15. Mager DE, Jusko WJ. General pharmacokinetic model for drugs exhibiting target-mediated drug disposition. *J Pharmacokinet Pharmacodyn.* 2001;28:507–532.
16. Levy G. Pharmacologic target-mediated drug disposition. *Clin Pharmacol Ther.* 1994;56:248–252.
17. Mager DE. Target-mediated drug disposition and dynamics. *Biochem Pharmacol.* 2006;72:1–10.
18. Mager DE, Krzyzanski W. Quasi-equilibrium pharmacokinetic model for drugs exhibiting target-mediated drug disposition. *Pharm Res.* 2005;22:1589–1596.
19. Gibiansky L, Gibiansky E, Kakkar T, Ma P. Approximations of the target-mediated drug disposition model and identifiability of model parameters. *J Pharmacokinet Pharmacodyn.* 2008;35:573–591.
20. Cancer de mama avanzado con el anticuerpo monoclonal hR3 en combinacion con doxorrubicina y ciclofosfamida. Fase I. The Cuban Clinical Trials Website. Registro Público Cubano de Ensayos Clínicos. http://www.registroclinico.sld.cu/ensayos/RPCEC00000057-Sp. Accessed June 26, 2014.
21. Advanced breast cancer with monoclonal antibody hR3 in combination with doxorubicin and cyclophosphamide. Phase I. http://rpcec.sld.cu/trials/RPCEC00000057-En. Accessed September 18, 2014.
22. Bauer R. *NONMEM users guide introduction to NONMEM 7.2. 0.* Ellicott City, MD: ICON Development Solutions; 2011.
23. Karlsson MO, Sheiner LB. The importance of modeling interoccasion variability in population pharmacokinetic analyses. *J Pharmacokinet Biopharm.* 1993;21:735–750.
24. Burnham KP, Anderson DR. *Model Selection and Multimodel Inference: A Practical Information-Theoretic Approach*. Springer; 2002.
25. Efron B. Bootstrap methods: another look at the jacknife. *Ann Stat.* 1979;7:26.
26. Glassman PM, Balthasar JP. Mechanistic considerations for the use of monoclonal antibodies for cancer therapy. *Cancer Biol Med.* 2014;11:20–33.

27. Ma P, Yang BB, Wang YM, et al. Population pharmacokinetic analysis of panitumumab in patients with advanced solid tumors. *J Clin Pharmacol.* 2009;49:1142–1156.
28. Dirks NL, Nolting A, Kovar A, Meibohm B. Population pharmacokinetics of cetuximab in patients with squamous cell carcinoma of the head and neck. *J Clin Pharmacol.* 2008;48:267–278.
29. Kuester K, Kovar A, Lüpfert C, Brockhaus B, Kloft C. Population pharmacokinetic data analysis of three phase I studies of matuzumab, a humanized anti-EGFR monoclonal antibody in clinical cancer development. *Br J Cancer.* 2008;98(5):900–906.
30. Fornier MN, Seidman AD, Schwartz MK, et al. Serum HER2 extracellular domain in metastatic breast cancer patients treated with weekly trastuzumab and paclitaxel: association with HER2 status by immunohistochemistry and fluorescence in situ hybridization and with response rate. *Ann Oncol.* 2005;16:234–239.
31. Dirks NL, Meibohm B. Population pharmacokinetics of therapeutic monoclonal antibodies. *Clin Pharmacokinet.* 2010;49:633–659.
32. Rivera F, Vega-Villegas ME, Lopez-Brea MF, Marquez R. Current situation of panitumumab, matuzumab, nimotuzumab and zalutumumab. *Acta Oncol.* 2008;47:9–19.
33. Bruno R, Washington CB, Lu JF, Lieberman G, Banken L, Klein P. Population pharmacokinetics of trastuzumab in patients with HER2+ metastatic breast cancer. *Cancer Chemother Pharmacol.* 2005;56:361–369.
34. Kuester K, Kovar A, Lüpfert C, Brockhaus B, Kloft C. Refinement of the population pharmacokinetic model for the monoclonal antibody matuzumab: external model evaluation and simulations. *Clin Pharmacokinet.* 2009;48(7):477–487.
35. Shi S. Biologics: an update and challenge of their pharmacokinetics. *Curr Drug Metab.* 2014;15:271–290.
36. Dostalek M, Gardner I, Gurbaxani BM, Rose RH, Chetty M. Pharmacokinetics, pharmacodynamics and physiologically-based pharmacokinetic modelling of monoclonal antibodies. *Clin Pharmacokinet.* 2013;52:83–124.
37. Fasanmade AA, Adedokun OJ, Olson A, Strauss R, Davis HM. Serum albumin concentration: a predictive factor of infliximab pharmacokinetics and clinical response in patients with ulcerative colitis. *Int J Clin Pharmacol Ther.* 2010;48:297–308.
38. Tongu M, Harashima N, Yamada T, Harada T, Harada M. Immunogenic chemotherapy with cyclophosphamide and doxorubicin against established murine carcinoma. *Cancer Immunol Immunother.* 2010;59:769–777.
39. Garrido G, Tikhomirov IA, Rabasa A, et al. Bivalent binding by intermediate affinity of nimotuzumab. *Cancer Biol Ther.* 2011;11:373–382.